Journal of Alloys and Compounds 619 (2015) 464–473

Contents lists available at ScienceDirect

Journal of Alloys and Compounds

journal homepage: www.elsevier.com/locate/jalcom

Ab initio study of the compound-energy modeling of multisublattice structures: The (hP6) Ni_2In-type intermetallics of the Ni–In–Sn system

S. Ramos de Debiaggi [a,b,*], N.V. González Lemus [a], C. Deluque Toro [c], A. Fernández Guillermet [d]

[a] Facultad de Ingeniería, Universidad Nacional del Comahue, Buenos Aires 1400, 8300 Neuquén, Argentina
[b] Instituto de Investigación y Desarrollo en Ingeniería de Procesos, Biotecnología y Energías Alternativas – CONICET-UNCo, Argentina
[c] Grupo de Nuevos Materiales, Universidad de la Guajira, Riohacha, Colombia
[d] CONICET - Instituto Balseiro, Centro Atómico Bariloche, Avda. Bustillo 9500, 8400 Bariloche, Argentina

ARTICLE INFO

Article history:
Received 9 July 2014
Received in revised form 23 August 2014
Accepted 25 August 2014
Available online 4 September 2014

Keywords:
Ni–In–Sn system
Ni_2In (hP6) sublattice model
Thermodynamic and electronic properties
Ab initio calculations
Lead-free soldering alloys
Intermetallics

ABSTRACT

The thermodynamic modeling of non-stoichiometric, multisublattice intermetallic phases using the Compound-Energy Formalism (CEF) involves the determination of parameters representing the Gibbs energy (G_m) of binary compounds, the so-called "end-member compounds" (EMCs), which are often metastable or hypothetical. In current CALPHAD (*i.e.*, "Calculation of Phase Diagrams") work, these quantities are treated as free parameters to be determined by searching for the best fit to the available information in the optimization procedure. The general purpose of this paper is to propose a theoretical approach to the study of the EMCs which makes use of density-functional-theory (DFT) *ab initio* calculations. The present method is applied to the EMCs involved in the CEF modeling of the non-stoichiometric (hP6) Ni_2In-structure type phase of the Ni–In and Ni–In–Sn systems using the three-sublattice models $(Ni)_1(Ni,Va)_1(In,Ni)_1$ and $(Ni,Va)_1(Ni,Va)_1(In,Ni,Sn)_1$, respectively. By means of systematic *ab initio* projected augmented waves (PAW) calculations using the VASP code we study the EMCs involved in the CEF formulations of the G_m for this phase in the binary and the ternary systems. Specifically, we study the twelve EMCs corresponding to the following sublattice occupations: $(Ni)_1(Ni)_1(In)_1$, which is usually described as Ni:Ni:In (*i.e.*, a compound with formula "Ni_2In"), Ni:Ni:Ni (*i.e.*, "Ni_3"), Ni:Ni:Sn ("Ni_2Sn"), Ni:Va:In (*i.e.*, "NiIn"), Ni:Va:Ni (*i.e.*, "Ni_2"), Ni:Va:Sn ("NiSn"), Va:Ni:In ("NiIn"), Va:Ni:Ni ("Ni_2"), Va:Ni:Sn ("NiSn"), Va:Va:In ("In"), Va:Va:Ni ("Ni"), and Va:Va:Sn ("Sn"). For the listed EMCs, we report the lattice-parameters, the volume per atom, the electronic density of states and various types of cohesive properties usually taken as macroscopic manifestations of the bonding strength, *viz.*, the bulk modulus and its pressure derivative, the cohesive energy and the energy of formation from the elements. Trends in these quantities are established as a function of the occupation of the various sublattices by the different components and discussed in terms of the interactions between d electrons of the transition element as well as the hybridization between them and the s and p electrons of the non-transition metal. In addition to the reported thermodynamic information of direct use as input in the CALPHAD optimizations, the picture of the variations in cohesive properties emerging from the present work should be useful in systematizing the thermophysical and structural database for this class of compounds.

1. Introduction

A traditional challenge of materials science is the accurate account of the thermodynamic stability of multicomponent alloys and compounds [1]. A usual phenomenological approach based upon classical and chemical thermodynamics is the so-called CALPHAD (*i.e.*, Calculation of Phase Diagrams) approach [2]. This method is aimed at producing a consistent thermodynamic description of the phase diagram and the thermochemical properties by constructing the Gibbs energy (G_m) functions of the various alloyed phases involved. The systematic application of the CALPHAD approach has shown that this technique might also be considered as a predictive tool. In particular, it has frequently been found that the G_m function of multicomponent substitutional alloys can be estimated by a suitable combination of the G_m descriptions for the lower-order systems, in particular, the descriptions of the binary and ternary subsystems. On the other hand, when treating

* Corresponding author. Address: Dpto. de Física. Facultad de Ingeniería, Universidad Nacional del Comahue, Buenos Aires 1400, 8300 Neuquén, Argentina. Tel.: +54 299 4490331; fax: +54 299 4490329.
E-mail address: susana.ramos@fain.uncoma.edu.ar (S. Ramos de Debiaggi).

http://dx.doi.org/10.1016/j.jallcom.2014.08.217
0925-8388/

ternary and higher-order intermetallic phases (IPs) with a usual formalism in CALPHAD work, *viz.*, the Compound-Energy Formalism (CEF) [3], it is necessary to determine parameters of the model representing the Gibbs energy of formation of binary compounds, the so-called "end-member compounds" (EMCs) [2] which are often metastable or hypothetical. Usually, these quantities are treated as free parameters to be determined by searching for the best fit to the available information on the phase diagram and the thermochemical properties, in particular, to calorimetric and activity data, using computer optimization methods [4]. In this way, the CALPHAD method leads to useful mathematical descriptions of the probable G_m functions. However, the experimental data on IPs are often scarce and insufficient for a reliable determination of the EMCs. As a consequence, there is a considerable interest in the development and testing of reliable predictive methods, to be used as complements of the CALPHAD optimizations, as well as for predicting, systematizing and interpreting the necessary thermodynamic information on EMCs with various formulas and structures.

The general purpose of the present paper is to explore the application of *ab initio* techniques to produce, systematize and interpret in microscopic terms various types of thermophysical properties of the EMCs involved in the CALPHAD modeling of a specific intermetallic phase of the Ni–In–Sn system. In the following we summarize the background and motivations of the study.

A practical motivation of the present work is the increasing interest in the design of lead-free soldering (LFS) alloys. Previous works by the present authors have been devoted to the theoretical prediction and systematization of thermodynamic properties of the binary IPs which are stable or metastable in systems considered as candidates for LFS applications, *viz.*, the Cu–In–Sn system [5] and the Ni–In–Sn system [6]. In these previous studies information was also obtained on the EMCs involved in the CEF modeling of several non-stoichiometric IPs. The present work goes one step forward in this line of research and focuses on the EMCs involved in the CEF modeling of a key non-stoichiometric phase of the Ni–In [7,8] and the Ni–In–Sn system [9] *viz.*, the (hP6) Ni_2In-structure type phase [10].

A theoretical motivation of the work is the long-standing interest in the possible uses of *ab initio* calculations in the CALPHAD environment [11,12]. In particular, Ansara et al. [11] discussed years ago the problems and difficulties arising in the CEF modeling of ordered IPs with various crystallographic sublattices. They noted that for a binary phase with "n" sublattices in which both type of atoms are allowed to enter each one of these sublattices, the application of the CEF involves the Gibbs energy of formation of 2^n EMCs. Even by introducing certain constraints between these quantities, the number of parameters corresponding to the EMCs would still remain too high in relation to the amount of experimental data. Therefore in current CALPHAD modeling work an approximation has often been introduced based on considering that different, but in some respect "similar" sublattices of the crystal structure, might be combined into one sublattice of the thermodynamic model. In view of this usual practice, Ansara et al. [11] attempted to provide some general criteria for combining sublattices by referring to the traditional "factors" in phenomenological alloy theory, such as the "size factor" and the "electronic factor" [13] and reviewed the methods available at that time to predict the Gibbs energy of formation of the EMCs.

In the present work an alternative approach to the study of multisublattice IPs, which makes use of *ab initio* density-functional theory (DFT) calculations, will be explored. The key features of the present methodology are the following. In the first place, the parameter-free *ab initio* calculations provide consistently thermodynamic quantities which may be adopted as inputs in the CEF modeling without approximations concerning the description of the structure. This fact makes it possible to preserve what it may be considered as the most attractive conceptual possibility of the CEF, *viz.*, the full coincidence between the actual crystallographic sublattices and the sublattices assumed in the thermodynamic model. In the second place, in addition to the thermodynamic quantities of direct use in the CALPHAD optimizations, the *ab initio* approach can be used to establish various types of cohesive properties of these EMCs, such as the cohesive energy and the bulk modulus, which are usually taken as macroscopic manifestations of the bonding strength. Finally, the present methodology also provides information on the electronic structure which can be used to develop a microscopic picture of the chemical bonding trends, and use that picture to interpret the variations in cohesive properties.

The methodology described above will be applied in the present work to the CEF modeling of the (hP6) Ni_2In-structure type phase. The stability of this phase in the Ni–In system was described by Waldner and Ipser [14] using a CEF model in which Ni atoms, In atoms and vacant (Va) crystal sites distribute themselves in three sublattices. By adopting the standard CEF notation and including in parentheses the components (*i.e.*, elements or Va) entering each sublattice, the Waldner and Ipser model may be described as $(Ni)_1(Ni,Va)_1(In,Ni)_1$ and we remark that the thermodynamic sublattices are directly based upon the crystallographic sublattices. Moreover, the related Ni_3Sn_2 (hP6) phase of the Ni–Sn system was modeled by Zemanova et al. using the three sublattice model $(Ni,Va)_1(Ni,Va)_1(Ni,Sn)_1$ [15]. Reports on the modeling of the G_m of this phase in the Ni–In–Sn ternary system have also been presented. In the first place, Zemanova et al. [16] proposed for this phase in the Ni–In–Sn system the three sublattice model $(Ni,Va)_1(Ni,Va)_1(In,Sn)_1$. More recently, in order to model this phase in the Ni–In–Sn system by allowing for complete solubility between the Ni_2In phase of the Ni–In binary and the Ni_3Sn_2 phase of the Ni–Sn binary, Schmetterer et al. [17] adopted the scheme $(Ni,Va)_1(Ni,Va)_1(In,Ni,Sn)_1$. Although the full details of their assessment work have not yet been published, the results in [17] indicate that the ternary experimental data a 973 K can be well accounted for by adopting the CEF to describe the (hP6) phase. This implies the use of a G_m function of the following type [2,3]:

$$\begin{aligned} G_m = {} & y^{\mathrm{I}}_{\mathrm{Ni}} y^{\mathrm{II}}_{\mathrm{Ni}} y^{\mathrm{III}}_{\mathrm{In}} {}^0G_{\mathrm{Ni:Ni:In}} + y^{\mathrm{I}}_{\mathrm{Ni}} y^{\mathrm{II}}_{\mathrm{Ni}} y^{\mathrm{III}}_{\mathrm{Ni}} {}^0G_{\mathrm{Ni:Ni:Ni}} + y^{\mathrm{I}}_{\mathrm{Ni}} y^{\mathrm{II}}_{\mathrm{Ni}} y^{\mathrm{III}}_{\mathrm{Sn}} {}^0G_{\mathrm{Ni:Ni:Sn}} \\ & + y^{\mathrm{I}}_{\mathrm{Ni}} y^{\mathrm{II}}_{\mathrm{Va}} y^{\mathrm{III}}_{\mathrm{In}} {}^0G_{\mathrm{Ni:Va:In}} + y^{\mathrm{I}}_{\mathrm{Ni}} y^{\mathrm{II}}_{\mathrm{Va}} y^{\mathrm{III}}_{\mathrm{Ni}} {}^0G_{\mathrm{Ni:Va:Ni}} + y^{\mathrm{I}}_{\mathrm{Ni}} y^{\mathrm{II}}_{\mathrm{Va}} y^{\mathrm{III}}_{\mathrm{Sn}} {}^0G_{\mathrm{Ni:Va:Sn}} \\ & + y^{\mathrm{I}}_{\mathrm{Va}} y^{\mathrm{II}}_{\mathrm{Ni}} y^{\mathrm{III}}_{\mathrm{In}} {}^0G_{\mathrm{Va:Ni:In}} + y^{\mathrm{I}}_{\mathrm{Va}} y^{\mathrm{II}}_{\mathrm{Ni}} y^{\mathrm{III}}_{\mathrm{Ni}} {}^0G_{\mathrm{Va:Ni:Ni}} + y^{\mathrm{I}}_{\mathrm{Va}} y^{\mathrm{II}}_{\mathrm{Ni}} y^{\mathrm{III}}_{\mathrm{Sn}} {}^0G_{\mathrm{Va:Ni:Sn}} \\ & + y^{\mathrm{I}}_{\mathrm{Va}} y^{\mathrm{II}}_{\mathrm{Va}} y^{\mathrm{III}}_{\mathrm{In}} {}^0G_{\mathrm{Va:Va:In}} + y^{\mathrm{I}}_{\mathrm{Va}} y^{\mathrm{II}}_{\mathrm{Va}} y^{\mathrm{III}}_{\mathrm{Ni}} {}^0G_{\mathrm{Va:Va:Ni}} + y^{\mathrm{I}}_{\mathrm{Va}} y^{\mathrm{II}}_{\mathrm{Va}} y^{\mathrm{III}}_{\mathrm{Sn}} {}^0G_{\mathrm{Va:Va:Sn}} \\ & - T\Delta^{\mathrm{M}}S_m + {}^{E}G_m \end{aligned} \quad (1)$$

In Eq. (1) the twelve ${}^0G_{i:j:l}$ quantities (with i,j,l = In,Ni,Sn,Va) represent the Gibbs energy of the EMCs (in kJ per mole of atoms), corresponding to the following sublattice occupations: $(Ni)_1(Ni)_1(In)_1$, which is usually described as Ni:Ni:In (*i.e.*, a compound with formula "Ni_2In"), Ni:Ni:Ni (*i.e.*, "Ni_3"), Ni:Ni:Sn ("Ni_2Sn"), Ni:Va:In (*i.e.*, "NiIn"), Ni:Va:Ni (*i.e.*, "Ni_2"), Ni:Va:Sn ("NiSn"), Va:Ni:In ("NiIn"), Va:Ni:Ni ("Ni_2"), Va:Ni:Sn ("NiSn"), Va:Va:In ("In"), Va:Va:Ni ("Ni"), and Va:Va:Sn ("Sn"). The energy part of these ${}^0G_{i:j:l}$ parameters, referred to the energy of the pure elements in their stable structures at 0 K will be determined in the following. The y_i^{φ} factors in Eq. (1) are the so-called site-fractions describing the occupation by the component i (with i = In,Ni,Sn,Va) in the sublattice φ (with φ = I,II,III), T is the temperature, $\Delta^{\mathrm{M}}S_m$ accounts for the ideal entropy of mixing of the components in the various sublattices and ${}^EG_m$ represents the excess Gibbs energy of the phase [3].

By means of systematic *ab initio* projected augmented waves (PAW) calculations [18,19] using the VASP code [20] we study the structural, cohesive properties and the electronic structure of the twelve EMCs involved in Eq. (1). Specifically, for these various EMCs we calculate *ab initio* the lattice-parameters, the volume per

atom, the bulk modulus and its pressure derivative, the cohesive energy, the energy of formation from the elements In, Ni and Sn in their stable structures and the electronic density of states. Trends in these quantities are established as a function of the occupation of the three sublattices by the different components of the alloy and discussed in the light of a theoretical picture of bonding for this class of compounds.

2. Phases and structures

The present *ab initio* treatment of the EMCs involved in the multi-sublattice models proposed for the Ni–In and the Ni–In–Sn system, was based on correlating the thermodynamic-model sublattices of the CEF with the actual crystallographic sublattices defined by sites sharing the same symmetrical Wyckoff positions. Specifically, to describe the Ni_2In phase in the Ni–In system and the Ni–In–Sn system we adopted the basic hP6 structure and identified the crystallographic sublattices comprising the Wyckoff sites 2*a*, 2*d* and 2*c* with the sublattices I, II and III thermodynamic sublattices, respectively, of the extended ternary three-sublattice model $(Ni,Va)_1(Ni,Va)_1(In,Ni,Sn)_1$ [17]. In Fig. 1 we present the structures of the Ni:Ni:M, Ni:Va:M and Va:Ni:M compounds with M = In.

3. Theoretical method

Spin polarized total energy DFT calculations were performed using the PAW method [18,19] and the VASP code [20]. For the exchange–correlation energy we adopted the generalized gradient approximation due to Perdew and Wang (GGA-PW91) [21]. For the PAWs we considered 10 valence electrons for Ni ($3d^8 4s^2$), 3 for In ($5s^2 p^1$) and 4 for Sn ($5s^2 p^2$). The kinetic energy cut-off for the plane wave expansion of the electronic wavefunction was 330 eV. The choice of the cutoff energy was tested upon the total energies and the energy of formation for the Ni_3In (hP8), a stable related compound of the Ni–In system, and the corresponding elements. Calculations performed using a cut-off energy of 450 eV led to changes in the total energy of less than 10 meV/atom (1 kJ/mol), with the energies of formation converged within 2 meV/atom (0.2 kJ/mol) when adopting a cut-off energy of 330 eV [6]. We used the Monkhorst–Pack *k*-point meshes [22] and the Methfessel–Paxton technique [23] with a smearing factor of 0.1 for the electronic levels. The convergence of the *k*-point meshes was checked until the energy converged with a precision better than 1 meV/atom. In this way the *k*-meshes considered were $19 \times 19 \times 15$ for Ni:Ni:M, $21 \times 21 \times 17$ for Ni:Va:M, $21 \times 21 \times 19$ for Va:Ni:M, and $21 \times 21 \times 13$ for Va:Va:M (with M = In, Sn). These values implied up to 480 *k* points in the irreducible Brillouin zone, depending on the specific EMC considered. The criterion for the self-consistent convergence of the total energy was 0.1 meV. The structures were optimized with respect to the lattice-parameters and the internal degrees of freedom compatible with the space group symmetry of the crystal structure, until the forces were less than 30 meV/Å and the energy variations with respect to the structural degrees of freedom were better than 1 meV/atom.

The total energy (E) and external pressure (P) were calculated for values of volume (V) varying slightly around the equilibrium (up to ±5%), relaxing all external and internal coordinates of the system. The bulk modulus an its pressure derivative were obtained by fitting the calculated pressure–volume values to the P vs V equation of state proposed by Vinet et al. [24].

The energy of formation (EOF) of the EMCs was calculated as:

$$\Delta E^{\varphi}(Ni_aM_b) = \frac{1}{a+b}E^{\varphi}_{Ni_aM_b} - \left[\frac{a}{a+b}E^{\theta}_{Ni} + \frac{b}{a+b}E^{\psi}_{M}\right] \quad (2)$$

where ΔE^{φ} is the EOF per atom of the Ni_aM_b (with M = In, Sn) compound with the structure φ, $E^{\varphi}_{Ni_aM_b}$ the corresponding total energy, E^{θ}_{Ni} is the total energy per atom of Ni in its equilibrium phase θ (fcc), and E^{ψ}_{M} is the total energy per atom of In or Sn in their equilibrium structure ψ (ψ = tI2 for In and tI4 for Sn [6]). This choice of the reference states allows a direct comparison of the theoretical EOF values with the results of calorimetric experiments and with the values derived in the CALPHAD modeling of phase diagrams, when available. A negative EOF means that the compound is thermodynamically stable with respect to the elements. This is the expected behavior of the compounds which are observed as stable phases at very low temperatures in the phase diagram.

As generally accepted [25] the cohesive energy (E_{coh}) of the EMCs was calculated as the difference between the total energy of the compound and the calculated atomic energy (E^{at}) of the isolated atoms present in the cell in their corresponding atomic electronic configuration *viz.*,

$$E^{\varphi}_{coh}(Ni_aM_b) = \left[\frac{a}{a+b}E^{at}_{Ni} + \frac{b}{a+b}E^{at}_{M}\right] - \frac{1}{a+b}E^{\varphi}_{Ni_aM_b} \quad (3)$$

4. Discussion

The calculated lattice-parameters, the equilibrium volume, the bulk modulus and its pressure derivative for the elements Ni, In and Sn in their known equilibrium structures have been reported elsewhere [6,26]. These results compare very well with the available experimental data and with other *ab initio* calculations. Such an agreement adds to the confidence on the present theoretical technique. In the following we present and discuss the results for the pure Ni, Ni–In and Ni–Sn EMCs.

4.1. Structural properties

The calculated properties of the pure Ni, Ni–In and Ni–Sn EMCs are listed in Table 1. In Table 2 we present the corresponding interatomic distances. The lattice-parameters (LPs) "*a*" and "*c*" and the volume per atom (V_o) are presented in Fig. 2 for the compounds with formulas "NiIn" and "Ni_2In" (Fig. 2a, d and g), "NiSn" and "Ni_2Sn" (Fig. 2b, e and h), "Ni_2" and "Ni_3" (Fig. 2c and i). The lines connecting the points are only to guide the eye thus making more evident the trends discussed here. The LPs of the group of EMCs containing In (*i.e.*, the Ni:Ni:In, Ni:Va:In and Va:Ni:In) are remarkable similar to those of the EMCs containing Sn (*i.e.*, the Ni:Ni:Sn, Ni:Va:Sn and Va:Ni:Sn, respectively), whereas the LPs of the compounds containing only Ni are smaller. Indeed, the same trend is shown by the cell volume (not shown), which might be correlated with the fact that the atomic radius of In (1.67 Å) and Sn (1.54 Å) are similar, whereas the atomic radius of Ni (1.25 Å) is significantly smaller. In each group of EMCs the "*a*" parameter decreases significantly when passing from a Ni:Ni:M compound to a Ni:Va:M compound (with M = In,Ni,Sn). It also decreases when passing from Ni:Ni:Ni to Va:Ni:Ni but increases when passing from Ni:Ni:M to Va:Ni:M (M = In,Sn). In the three groups of EMCs the "*c*" parameter

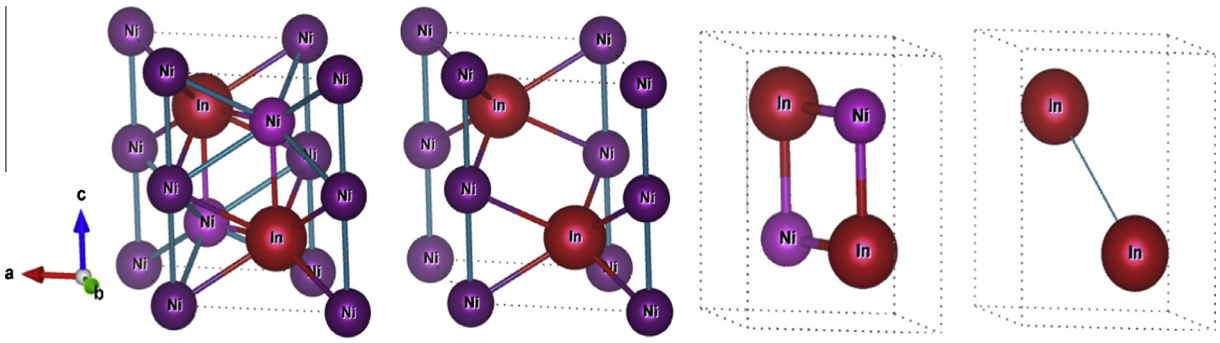

Fig. 1. Structures of the EMCs for the Ni_2In (hP6) structure type phase. From left to right: Ni:Ni:In, Ni:Va:In, Va:Ni:In, Va:Va:In.

Table 1
Ab initio lattice parameters, (a and c), equilibrium volume per atom (V_o), bulk modulus (B_o), and its pressure derivative (B_o'), cohesive energy (E_{coh}) and energy of formation (EOF) from the elements for the end members compounds (EMCs) described by the given sublattice-occupation schemes.

Sublattice occupation scheme	EMC formula	a, c (Å)	c/a	V_o (Å^3/at.)	B_o (Gpa)	B_o'	E_{coh} (kJ/mole)	EOF (kJ/mole)
Ni:Ni:In	"Ni_2In"	4.312 5.266	1.221	14.132	143.2	4.7	412.481	−4.689
		4.265[a] *5.163*[a]		*13.556*[a]				*−16.314*[b] *−17.339*[c]
		4.317[d] *5.273*[d]		*14.183*[d]	*135.9*[d]	*2.9*[d]		
Va:Ni:In	"NiIn"	4.452 5.065	1.138	21.734	64.3	4.0	336.034	28.028
Ni:Va:In	"NiIn"	4.032 5.098	1.264	17.942	95.2	3.5	371.338	−7.214
Va:Va:In	"In"	3.400 5.535	1.628	27.712	36.1	4.7	232.621	0.474 *43.036*[b]
Ni:Ni:Sn	"Ni_2Sn"	4.292 5.301	1.235	14.094	146.7	4.5	450.606	−17.365 *−27.912*[b]
		4.306[e] *5.299*[e]		*14.189*[e]	*144.5*[e]	*4.4*[e]		*−15.490*[e]
Va:Ni:Sn	"NiSn"	4.445 4.996	1.124	21.374	73.8	5.0	395.500	6.733 *2.500*[b]
Ni:Va:Sn	"NiSn"	3.985 5.095	1.278	17.514	114.0	4.7	429.943	−27.640 *−26.089*[b]
		4.001[e] *5.102*[e]		*17.666*[e] *17.548*[f]	*108.6*[e] *109.3*[f]	*4.8*[e] *4.9*[f]		*−26.160*[e] *−27.427*[f]
Va:Va:Sn	"Sn"	3.810 4.602	1.208	28.924	44.2	4.0	299.508	9.857 *20.000*[b]
Ni:Ni:Ni	"Ni_3"	3.992 4.838	1.212	11.128	186.6	3.4	483.369	11.757 *17.564*[b] *15.725*[g]
Va:Ni:Ni	"Ni_2"	3.896 4.612	1.189	15.156	92.5	6.1	406.799	88.327 *15.725*[g]
Ni:Va:Ni	"Ni_2"	3.536 4.759	1.346	12.883	141.4	4.8	445.124	50.001 *17.564*[b] *15.725*[g]
Va:Va:Ni	"Ni"	2.480 4.094	1.650	10.906	191.9	3.7	489.399	5.728 *15.725*[g]

[a] Experimental data [10].
[b] CALPHAD [14].
[c] Experimental data at 298.15 K [29].
[d] Ferromagnetic (FM) FP-LAPW GGA-PBE and LDA-PW calculations including relaxations of internal coordinates [26].
[e] *Ab initio* USPP (Sn valence configuration including 4d electrons) [35].
[f] *Ab initio* USPP (alternative Sn valence configuration including only $5s^2p^2$ electrons) [35].
[g] CALPHAD [15].

decreases when passing from a Ni:Ni:M compound to a Ni:Va:M compound (with M = In,Ni,Sn) and also when passing from a Ni:Ni:M to Va:Ni:M (M = In,Ni,Sn) compound.

In order to compare with the trends in the cohesive properties (see below), we plot in Fig. 2g, h and i the volume per atom V_o. In each group of EMCs V_o increases slightly when passing from a Ni:Ni:M compound to a Va:Ni:M compound (with M = In,Sn), *i.e.*, when the sublattice I, corresponding to the Wyckoff positions 2*a* (Table 2 and Fig. 1) is filled with Va. When passing from Ni:Ni:M to Ni:Va:M (with M = Ni,In,Sn), *i.e.*, when sublattice II, corresponding to the Wyckoff positions 2*d* is filled with Va, the decrease in the volume per atom V_o is larger. These trends suggest that V_o of each group of EMCs is controlled in the first place by the occupation of the sites corresponding to the Wyckoff positions 2*d* and in the second place by those in the 2*a* positions. Although not shown here, and due to the LPs variations, the cell volume always decrease when passing from a Ni:Ni:M compound to a Ni:Va:M compound (with M = Ni,In,Sn). When passing from Ni:Ni:M to Va:Ni:M (with M = Ni,In,Sn) compound, it increases only slightly for M = In,Sn, but decreases for M = Ni.

4.2. Bulk modulus, cohesive energy and energy of formation

The composition dependence of the bulk modulus (B_o), the cohesive energy (E_{coh}) and the energy of formation (EOF) is represented in Fig. 3. When comparing the properties of the three groups of compounds, we find that B_o and E_{coh} decrease when passing from the group of EMCs containing only Ni to that with Sn and then to the EMCs containing In. In each group of EMCs B_o and E_{coh} decrease significantly when passing from the Ni:Ni:M compound (with M = Ni,In,Sn) to the Va:Ni:M compound. The decrease is smaller when passing from Ni:Ni:M to Ni:Va:M. These effects might be correlated with decreases in the number of Ni–Ni and Ni–M (M = In,Sn) interatomic bonds established by Ni atoms (Table 2). The results in Table 2 suggest that B_o and E_{coh} of the present compounds depend, in the first place, upon the Ni–Ni and Ni–M (M = In,Sn) interatomic bonds established by Ni atoms in the 2*d* Wyckoff positions, and, in the second place, upon those established by Ni atoms in the 2*a* positions.

We close this section by referring to the energy of formation (EOF) values for the present EMCs (Fig. 2g, h and i) We note, in

Table 2
Calculated interatomic distances and number of bonds for $(Ni,Va)_1$ $(Ni,Va)_1$ $(In,Ni, Sn,)_1$ EMCs.

Sublattice occupation scheme	Bond type	Wyckoff position and sublattice number					
		2*a* (I)		2*d* (II)		2*c* (III)	
		Number of bonds	Average distance	Number of bonds	Average distance	Number of bonds	Average distance
Ni:Ni:In	Ni–Ni	8	2.77	6	2.82	–	–
	Ni–In	6	2.82	5	2.55	11	2.70
	In–In	–	–	–	–	5	3.62
	Ni–Ni	–	–	–	–	–	–
Va:Ni:In	Ni–In	–	–	5	2.55	5	2.55
	In–In	–	–	–	–	6	3.61
	Ni–Ni	2	2.55	–	–	–	–
Ni:Va:In	Ni–In	6	2.65	–	–	6	2.65
	In–In	–	–	–	–	6	3.45
Va:Va:In	In–In	–	–	–	–	6	3.39
	Ni–Ni	8	2.77	6	2.81	–	–
Ni:Ni:Sn	Ni–Sn	6	2.81	5	2.55	11	2.69
	Sn–Sn	–	–	–	–	5	3.63
	Ni–Ni	–	–	–	–	–	–
Va:Ni:Sn	Ni–Sn	–	–	5	2.54	5	2.54
	Sn–Sn	–	–	–	–	6	3.58
	Ni–Ni	2	2.55	–	–	–	–
Ni:Va:Sn	Ni–Sn	6	2.63	–	–	6	2.63
	Sn–Sn	–	–	–	–	6	3.43
Va:Va:Sn	Sn–Sn	–	–	–	–	6	3.18
Ni:Ni:Ni	Ni–Ni	14	2.57	11	2.48	11	2.48
Va:Ni:Ni	Ni–Ni	–	–	5	2.27	5	2.27
Ni:Va:Ni	Ni–Ni	8	2.36	–	–	6	2.36
Va:VaNi	Ni–Ni	–	–	–	–	6	2.50

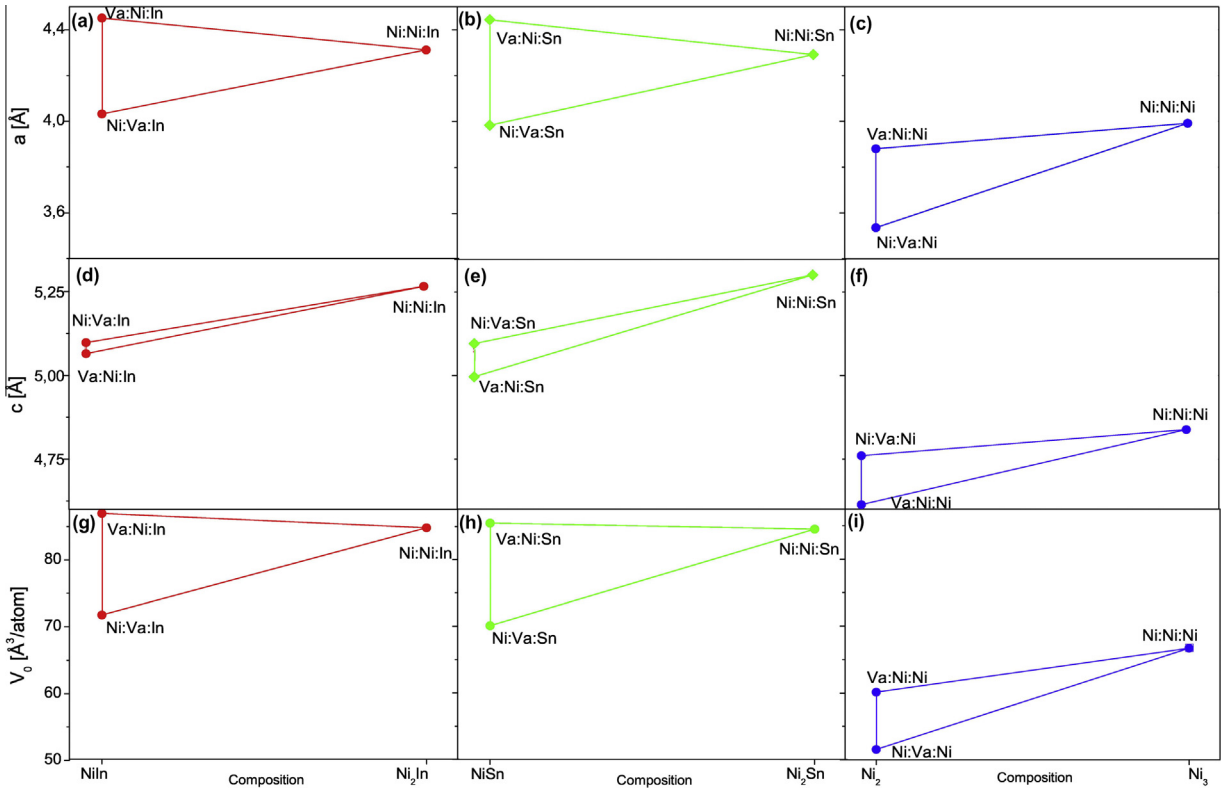

Fig. 2. Lattice parameters (*a* and *c*) and volume per atom (V_o) for the $(Ni,Va)_1$ $(Ni,Va)_1$ $(In,Ni,Sn)_1$ EMCs.

the first place that only the Ni:Ni:M and Ni:Va:M compounds (with M = In,Sn) are thermodynamically stable with respect to the elements in their stable structures (Table 1). In addition, the plots of –EOF versus composition for the groups of compounds containing In or Sn (Fig. 3g and h) show approximately similar trends, whereas the compounds of Ni (Fig. 3(i)) are less stable. In Fig. 4 we compare

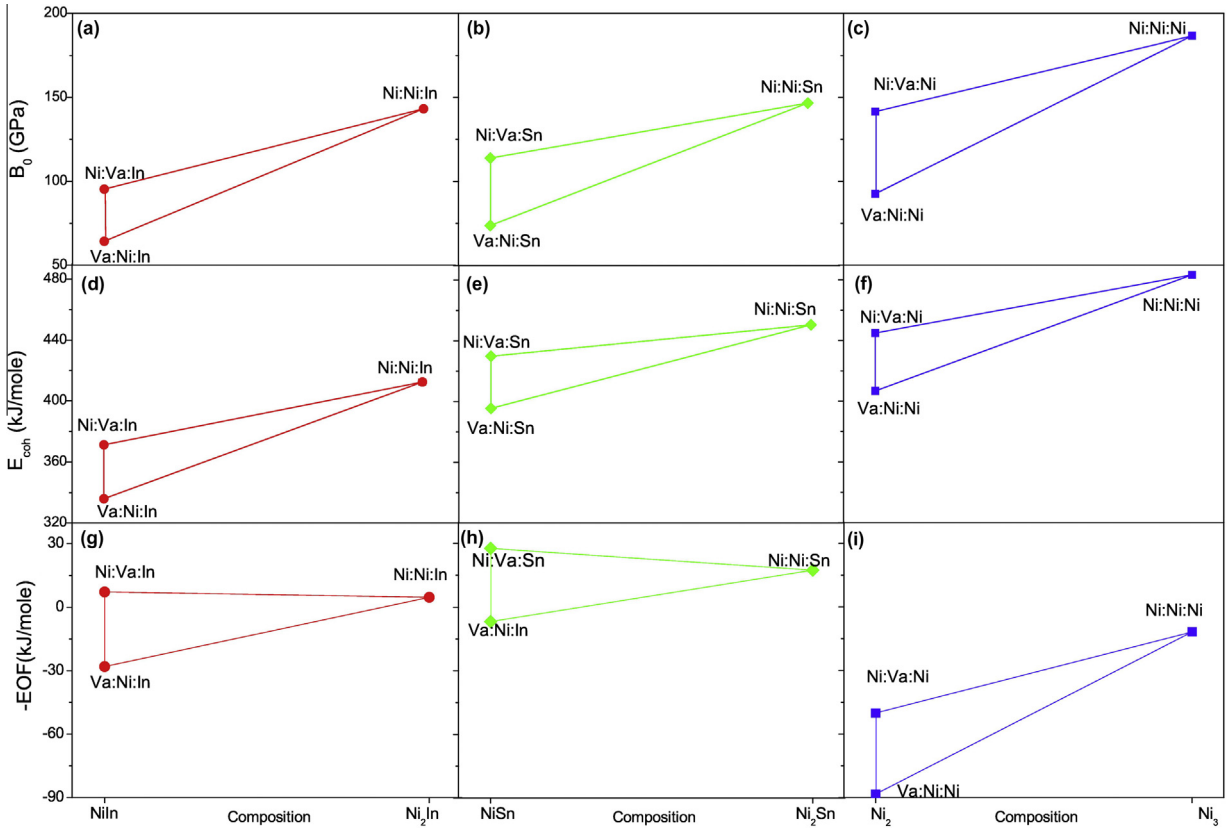

Fig. 3. Bulk modulus (B_o), cohesive energy (E_{coh}) and the negative energy of formation (–EOF) for the $(Ni,Va)_1$ $(Ni,Va)_1$ $(In,Ni,Sn)_1$ EMCs.

the *ab initio* calculated EOF for the EMCs with the values obtained in CALPHAD modeling works [14,15]. We note that most of the CALPHAD generated EOFs fall in a scatter band of ± 15 kJ/mol around the present *ab initio* results. The only exceptions are the EOF values for two Ni structures, *viz.*, Ni:Va:Ni and Va:Ni:Ni, and the Va:Va:In structure. A comparison with previously *ab initio* calculated EOF values is given in Table 1. These results [27–29] indicate a similar level of deviations between *ab initio* and CALPHAD as well as experimental results for related intermetallic systems. The origin of such deviations for these type of intermetallic systems is unknown. In view of this problem, we are currently working in evaluating *ab initio* the temperature contribution to the EOFs in order to determine if this contribution can explain, at least partly, the differences found between the 0 K *ab initio* values and the experimental (or CALPHAD generated) results at room temperature.

Finally we note that, in contrast to the previous CALPHAD modeling works [14,15]. the present *ab initio* calculations predict significant differences between the EOF "per atom" of the EMCs which are, in fact, different structures of pure Ni. In this sense the present results provide useful information that could be taken into consideration to improve future CALPHAD type optimizations of the Ni–In, Ni–Sn and Ni–In–Sn system.

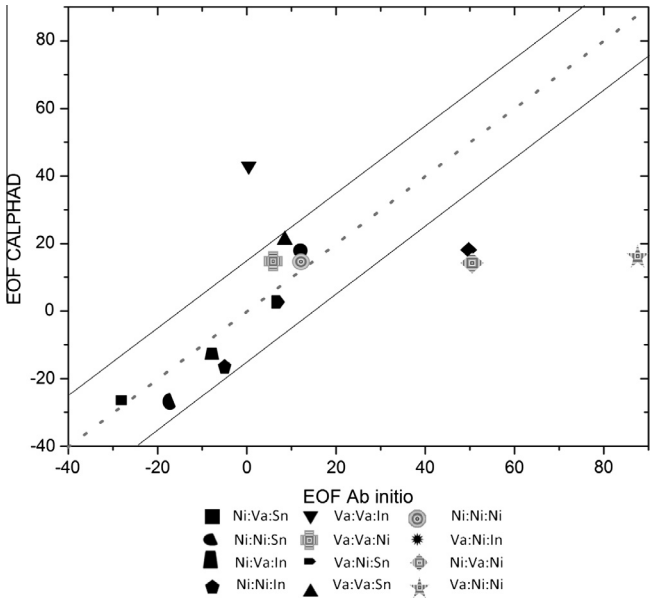

Fig. 4. Comparison between the *ab initio* calculated and CALPHAD generated values for the energy of formation (EOF) of EMCs (black [14], grey [15]).

4.3. Electronic density of states

In previous studies the present authors [6,26] analyzed the electronic density-of-states (DOS) of various stable and metastable Ni–In and Ni–Sn stoichiometric phases in terms of the d-electron contributions from the transition metal and the s and p contributions of In and Sn. In the present work we will extend the discussion to the DOS and the bonding characteristics of the EMCs involved in the CEF modeling of the (hP6) Ni_2In structure type phase of the Ni–In–Sn system. To this end we will rely mainly on the theory by Gelatt et al. [30], although other studies of the relations between the DOS and the properties of the IPs will also be considered [31–34].

The calculated DOS for the Ni:Ni:M, Ni:Va:M and Va:Ni:M compounds with M = In,Sn are compared in Fig. 5 with those structures with M = Ni. These comparisons suggest, in the first place, that the DOS of both the Ni:Ni:M and that of the Ni:Va:Sn compounds look

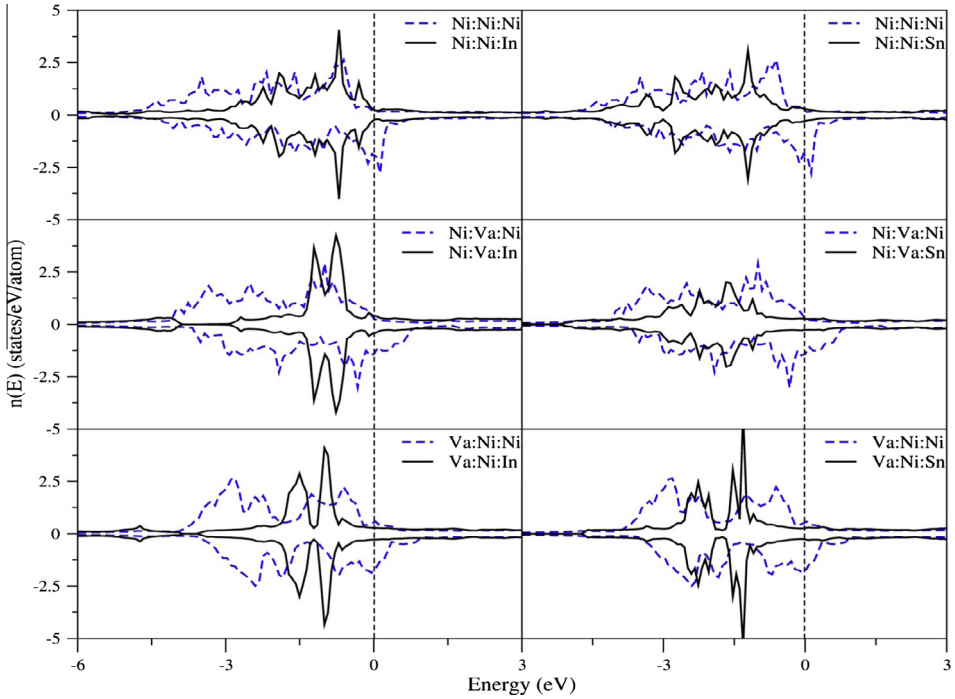

Fig. 5. Density of states for the Ni–In and Ni–Sn EMCs (solid lines) compared with the corresponding pure Ni structures (dashed lines).

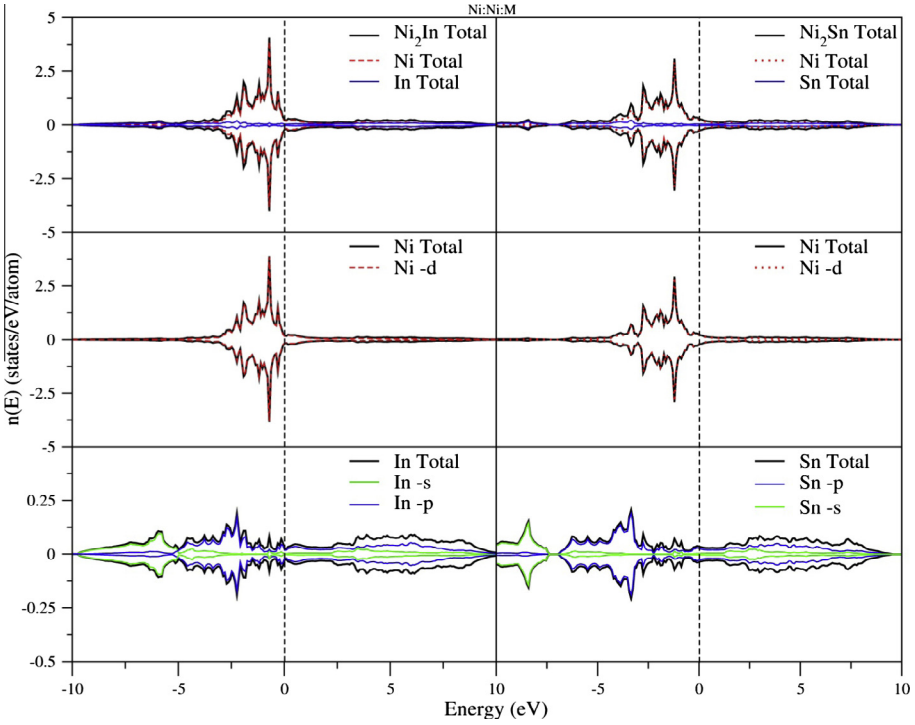

Fig. 6. Density of states for the Ni:Ni:In and Ni:Ni:Sn EMCs.

roughly similar to the DOS of Ni in the corresponding (non-stable) structures with a considerable reduction in the band width, although the structure and relative intensities of the peaks are different. Such reduction might be explained as the result of two contributions. The first contribution is the lattice expansion produced by the incorporation of the non-transition element, highlighted by Gelatt et al. [30]. This contribution is expected to be more important for In than for Sn compounds because the atomic volume of the former is larger (Table 1). The second contribution to the narrowing of the band width is the decrease in the number of Ni–Ni bonds (Table 2).

The comparisons in Fig. 5 also suggest that the DOS of Ni:Va:In as well as that of the Va:Ni:M (M = In,Sn) compounds differ qualitatively from that of the corresponding pure-Ni structures, which might reflect the effect of hybridization of the electronic orbitals of Ni with those of In and Sn [30]. In order to test this possibility

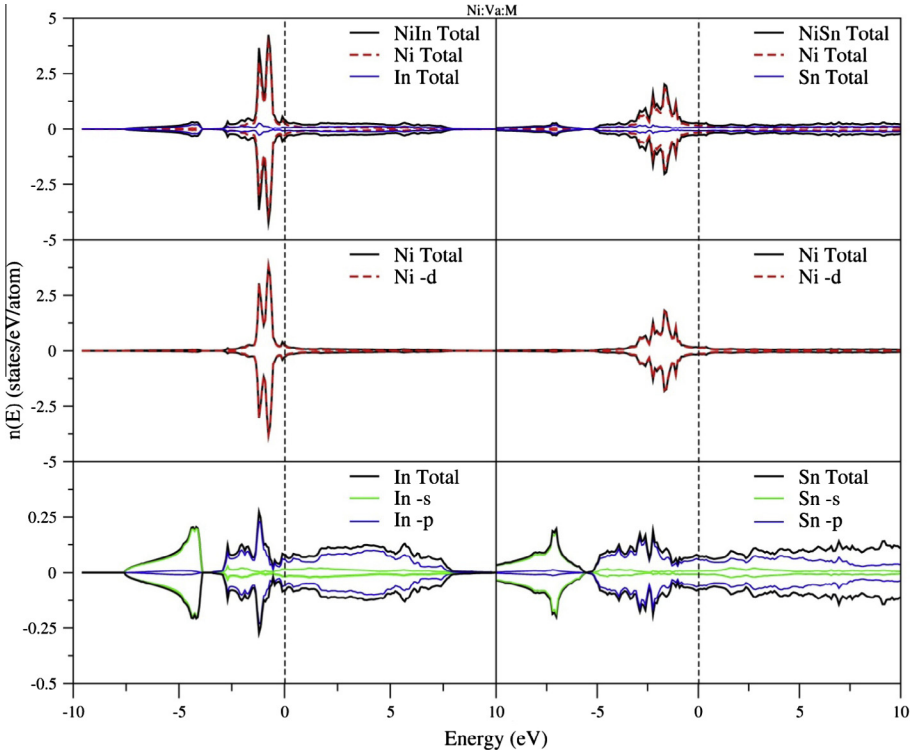

Fig. 7. Density of states for the Ni:Va:In and Ni:Va:Sn EMCs.

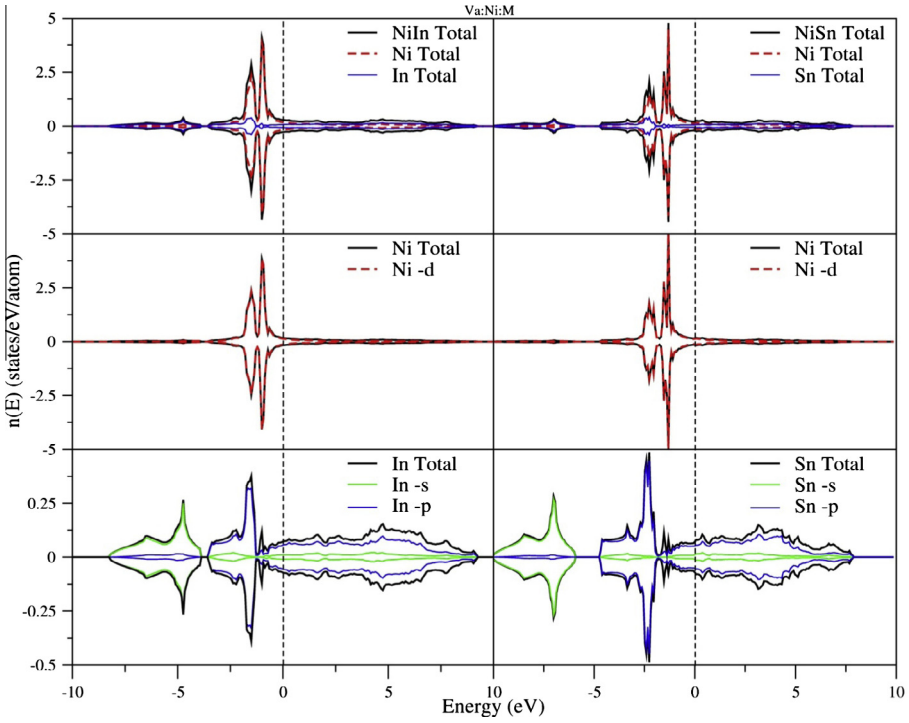

Fig. 8. Density of states for the Va:Ni:In and Va:Ni:Sn EMCs.

we plot in Figs. 6–8 the electron contributions for Ni and s and p contributions for In and Sn corresponding to the DOS of the Ni:Ni:M, Ni:Va:M and Va:Ni:M compounds (with M = In,Sn), respectively.

Fig. 6 suggests that the general features for the DOS of the Ni:Ni:M (M = In,Sn) compounds are determined by the Ni 3d-electrons. There are also minor contributions of 5s and 5p In or Sn orbitals whose bottom bands lie deeper in energy with respect to the Fermi energy (E_F). The s-band appears at lower energies and is clearly separated from the p-band, which extends to energies higher that the Fermi level.

Fig. 7 show that the DOS of the Ni:Va:M compounds is also dominated by the Ni-3d band contributions, with hybridization effects between the Ni-3d and (In,Sn)-5p electronic orbitals which

are more noticeable for Ni:Va:In. The DOS of this compound shows very narrow occupied bands, splitted in three parts separated by two pseudogaps. A pseudogap generally marks a position in energy which divides regions of bonding, non-bonding or antibonding states [30,34]. In the present case the Fermi level is placed in a region of possible antibonding character (see below). Fig. 8 shows similar effects upon the DOS of both Va:Ni:In and Va:Ni:Sn compounds. In all cases considered the DOS reveal metallic and non-magnetic behavior.

5. Correlation of cohesive properties and electronic structure

The characterization of the electronic structure discussed in the previous section will be used in the following to develop a microscopic interpretation of the calculated trends in cohesive properties. First of all, the fact that B_o and E_{coh} are the largest for the Ni:Ni:Ni compound might be correlated with the band-narrowing effect (which affects the Ni–Ni interactions) and the decrease in the number of Ni–Ni bonds caused by the presence of the non-transition metal element. Since the band-narrowing effect is larger for the compounds with In, the decrease in their cohesive properties is larger than for the compounds with Sn. Besides, by comparing the Ni:Ni:In with the Ni:Ni:Sn compounds we note that for the latter the main band spreads and shifts to lower energies, therefore increasing the bonding and cohesion of this compound with respect to Ni:Ni:In.

The incorporation of Va in the structure leads to the Va:Ni:M and Ni:Va:M compounds, which exhibit a larger volume per atom that the pure Ni compounds (Fig. 2). Consequently the cohesive properties decrease with respect to the Ni:Ni:M compounds, also as a consequence of the reduction of the number of Ni–Ni bonds. In addition, the calculated decrease in cohesive properties is more important when passing from the Ni:Ni:M to the Va:Ni:M compounds than when passing to the Ni:Va:M compounds. In the Ni:Va:In compound the Fermi level lies close to a peak of low intensity in the DOS, whereas for the Va:Ni:In compound the Fermi energy shifts to higher energies and more states of probable antibonding character are occupied, thus disfavouring the cohesion in Va:Ni:In with respect to that in Ni:Va:In. For the Ni:Va:Sn compound, the 3d-band is more spread and similar to that of the Ni:Ni:Sn compound, which may explain the higher cohesion of this compound compared to that of Va:Ni:Sn.

We close this section by referring to previous attempts to correlate the cohesive and stability properties of intermetallics with the position of the Fermi level in the DOS. In particular, Ravindran and Asokamani [34] suggested that the structural stability of an intermetallic compound may be correlated with the E_F lying in a pseudogap. This generalization would be consistent with the present interpreted DOS as long as a pseudogap often divides the DOS in regions of bonding and antibonding states, the filling of which affects the bonding properties of the (single phase) compound. According to Fig. 6 the E_F of the Ni:Ni:In compound falls at a small pseudogap, whereas for the Ni:Ni:Sn compounds a similar pseudogap is observed but at a lower energy. However, the cohesive properties of these compounds are similar and this precludes a test of the Ravindran and Asokamani correlation.

6. Summary and concluding remarks

The general purpose of this work is to contribute to the development of a method of analysis appropriate to produce, systematize and interpret a rather complete database with information on the compounds involved in the phenomenological (CALPHAD-type) modeling of the non-stoichiometric (hP6) Ni_2In structure-type phase of the Ni–In and Ni–In–Sn systems. These multisublattice phases have been treated using the Compound-Energy Formalism (CEF) using the schemes $(Ni)_1(Ni,Va)_1(In,Ni)_1$ [14] and $(Ni,Va)_1(Ni,Va)_1(In,Ni,Sn)_1$ [17], respectively. The Gibbs models developed in the framework of the CEF on the basis of the given schemes involve various stable, metastable and non-stable compounds (*i.e.*, the so-called end-member compounds, EMCs), the properties of which are in general not known from experiments, *viz.*, the hP6 structure compounds with formulas "Ni_2In", "NiIn" (2 EMCs), "Ni_3" and "Ni_2" (2 EMCs), "Ni", "Ni_2Sn", "NiSn" (2 EMCs), "In" and "Sn". The specific purpose of the present work is to obtain structural, cohesive, thermodynamic and electronic structure information on these EMCs using *ab initio* density-functional theory calculations.

Using the projector-augmented-wave method and the exchange and correlation functions of Perdew and Wang in the generalized gradient approximation [21], we calculated the lattice-parameters, volume per atom, bulk modulus and its pressure derivative, the cohesive energy, the energy of formation from the elements and the electronic density of states of the given EMCs. The results were used to establish trends in the effect upon the structural and cohesive properties, as well as the electronic density of states, of the filling up with Ni (or vacancies, Va) of the first (I) and second (II) sublattices, and the filling up with In, Ni or Sn of the third (III) sublattice of the CEF models.

The trends in the cohesive properties are analyzed in the light of a picture of the bonding characteristics of the present compounds which involves three key factors: (i) the variation in the number of Ni–Ni and Ni–M (M = In,Sn) bonds; (ii) the band narrowing effect caused by the incorporation of the non-transition element in the structure of the pure Ni compounds (*viz.*, the Ni:Ni:Ni, Ni:Va:Ni and Va:Ni:Ni EMCs); and, (iii) the effect of the hybridization of the d electronic states of Ni with the s and p electronic states of In or Sn. On this basis, the effects of filling up of the various sublattices with In, Ni, Sn or vacancies are discussed.

In conclusion, the present methodology yields information of direct use as input in the CALPHAD optimizations as well as a picture of the variations in cohesive properties which should be useful in systematizing the thermophysical and structural database for this class of compounds.

Acknowledgements

This work was supported by Project PIP 112-20110100814 from CONICET and Project I157 from Universidad Nacional del Comahue.

References

[1] M. Hillert, Phase Equilibria, Phase Diagrams and Phase Transformations, Cambridge University Press, Cambridge, UK, 1998.
[2] L. Kaufman, H. Bernstein, Computer Calculation of Phase Diagrams, Academic Press, New York, 1970.
[3] M. Hillert, The compound energy formalism, J. Alloys Comp. 330 (2001) 161–176.
[4] A. Fernández Guillermet, Assessment of phase stability and thermochemistry of high-melting alloys and compounds: a systematic approach based on Gibbs energy modelling, in: K.E. Spear (Ed.), Proc. Ninth International Conference on High Temperature Materials Chemistry, The Electrochemical Society Proceedings Pennington, New York, 1997, pp. 135–144.
[5] S. Ramos de Debiaggi, C. Deluque Toro, G.F. Cabeza, A. Fernández Guillermet, Ab initio comparative study of the Cu–In and Cu–Sn intermetallic phases in Cu–In–Sn alloys, J. Alloy. Comp. 542 (2012) 280–292.
[6] S. Ramos de Debiaggi, C. Deluque Toro, G.F. Cabeza, A. Fernández Guillermet, Ab initio study of the cohesive properties, electronic structure and thermodynamic stability of the Ni–In and Ni–Sn intermetallics, J. Alloys Comp. 576 (2013) 302–316.
[7] M.F. Singleton, P. Nash, in: T. Massalski (Ed.), Binary Alloys Phase Diagrams, ASM, The Materials Information Society, 1990.
[8] Ph. Durussel, G. Burri, P. Feschotte, The binary system Ni–In, J. Alloys Comp. 257 (1997) 253–258.
[9] C. Huang, S. Chen, Interfacial reactions in In–Sn/Ni couples and phase equilibria of the In–Sn–Ni system, J. Electron. Mater. 31 (2002) 152–160.

[10] P. Villars, Pearson's, in: A. Desk Edition (Ed.), Handbook of Crystallographic Data for Intermetallic Phases, vol. 2, ASM International, Materials Park, OH, USA, 1997, p. 2189.
[11] I. Ansara, T.G. Chart, A. Fernández Guillermet, F.H. Hayes, U.R. Kattner, D.G. Pettifor, N. Saunders, K. Zeng, Thermodynamic modelling of selected topologically close-packed intermetallic compounds, CALPHAD 21 (1997) 171–218.
[12] B.P. Burton, N. Dupin, S.G. Fries, G. Grimvall, A. Fernández Guillermet, A.P. Miodownik, W.A. Oates, V. Vinograd, Using ab initio calculations in the CALPHAD environment, Z. Metallkd. 92 (2001) 514–525.
[13] C.S. Barrett, T.B. Massalski, in: M. Hill (Ed.), Structure of Metals, McGraw-Hill Book Company, New York, 1966.
[14] P. Waldner, H. Ipser, Thermodynamic modeling of the Ni–In system, Z. Metallkd. 93 (2002) 825–832.
[15] A. Zemanova, A. Kroupa, A. Dinsdale, Theoretical assessment of the Ni–Sn system, Monatsh. Chem. 143 (2012) 1255–1261.
[16] A. Zemanova, A. Kroupa, R. Mishra, H. Ipser, H. Flandorfer, Thermodynamic assessment of the Ni–Sn–X (X=In, Sb) ternary systems, in: XL CALPHAD Conference, Rio de Janeiro, Brazil, 2011.
[17] C. Schmetterer, A. Zemanova, H. Flandorfer, A. Kroupa, H. Ipser, Phase equilibria in the ternary In–Ni–Sn system at 700 °C, Intermetallics 35 (2013) 90–97.
[18] P.E. Blöchl, Projector augmented-wave method, Phys. Rev. B 50 (1994) 17953–17979.
[19] G. Kresse, J. Joubert, From ultrasoft pseudopotentials to the projector augmented-wave method, Phys. Rev. B 59 (1999) 1758–1775.
[20] G. Kresse, J. Furthmüller, Efficiency of ab-initio total energy calculations for metals and semiconductors using a plane-wave basis set, Comput. Mater. Sci. 6 (1996) 15–50.
[21] J.P. Perdew, Y. Wang, Accurate and simple analytic representation of the electron-gas correlation energy, Phys. Rev. B 45 (1992) 13244–13249.
[22] H.J. Monkhorst, J.D. Pack, Special points for Brillouin-zones integrations, Phys. Rev. B 13 (1976) 5188–5192.
[23] M. Methfessel, A.T. Paxton, High-precision sampling for Brillouin-zone integration in metals, Phys. Rev. B 40 (1986) 3616–3621.
[24] P. Vinet, J.H. Rose, J. Ferrante, J.R. Smith, J. Phys, Universal features of the equation of the state of solids, Phys.: Condens. Matter 1 (1989) 1941–1963.
[25] R.A. Evarestov, Quantum Chemistry of Solids: The LCAO First Principles Treatment of Crystals, Springer Science & Business Media, 2007. p. 574.
[26] C. Deluque Toro, S. Ramos de Debiaggi, A.M. Monti, Study of cohesive, electronic and magnetic properties of the Ni–In intermetallic system, Physica B 407 (2012) 3236–3239.
[27] G. Ghosh, M. Asta, First-principles calculation of structural energetics of Al–TM (TM = Ti, Zr, Hf) intermetallics, Acta Mater. 53 (2005) 3225–3252.
[28] G. Ghosh, M. Asta, Phase stability, phase transformations, and elastic properties of Cu_6Sn_5: ab initio calculations and experimental results, J. Mater. Res. 20 (2005) 3102–3117.
[29] J. Schmid, M. Bienzle, F. Sommer, B. Predel, Thermodynamic study of solid and liquid Ni–In alloys, Z. Metallkd. 86 (1995) 877–881.
[30] C.D. Gelatt Jr., A.R. Williams, V.L. Moruzzi, Theory of bonding of transition metals to nontransition metals, Phys. Rev. B 27 (1983) 2005–2013.
[31] T. Hong, T.J. Watson-Yang, X.Q. Guo, A.J. Freeman, T. Orguchi, J. Xu, Crystal structure, phase stability, and electronic structure of Ti–Al intermetallics: Ti_3Al, Phys. Rev. B 43 (1991) 1994.
[32] J. Xu, A.J. Freeman, Band filling and structural stability of cubic trialuminides: YAl_3, $ZrAl_3$ and $NbAl_3$, Phys. Rev. B 40 (1989) 11927–11930.
[33] J. Xu, A.J. Freeman, Phase stability and electronic structure of $ScAl_3$, and $ZrAl_3$ and of Sc-stabilized cubic $ZrAl_3$ precipitates, Phys. Rev. B 41 (1990) 12553–12561.
[34] P. Ravidran, R. Asokamani, Correlation between electronic structure, mechanical properties and phase stability in intermetallic compounds, Bull. Mater. Sci. 20 (4) (1997) 613–622.
[35] G. Ghosh, First-principles calculation of phase stability and cohesive properties of Ni–Sn intermetallics, Metall. Mater. Trans. A 40 (2009) 4–23.